Historical variability and lifecycles of North Atlantic midlatitude cyclones originating in the tropics

Baker, A. J. ORCID: https://orcid.org/0000-0003-2697-1350, Hodges, K. I., Schiemann, R. K. H. and Vidale, P. L. (2021) Historical variability and lifecycles of North Atlantic midlatitude cyclones originating in the tropics. Journal of Geophysical Research: Atmospheres, 126 (9). e2020JD033924. ISSN 2169-8996 doi: https://doi.org/10.1029/2020JD033924 Available at https://centaur.reading.ac.uk/97427/

JGR Atmospheres

RESEARCH ARTICLE
10.1029/2020JD033924

Historical Variability and Lifecycles of North Atlantic Midlatitude Cyclones Originating in the Tropics

Alexander J. Baker[1], Kevin I. Hodges[1], Reinhard K. H. Schiemann[1], and Pier Luigi Vidale[1]

[1]National Centre for Atmospheric Science and Department of Meteorology, University of Reading, Reading, Berkshire, UK

Key Points:

- North Atlantic cyclones originating in the tropics examined across seven reanalyses
- Reanalyses show consistent interannual variability, seasonality, and structural evolution of tropical-origin cyclones
- Intensity evolution and tracks are distinct between warm-core and cold-core cyclones

Supporting Information:

Supporting Information may be found in the online version of this article.

Correspondence to:

A. J. Baker,
alexander.baker@reading.ac.uk

Citation:

Baker, A. J., Hodges, K. I., Schiemann, R. K. H., & Vidale, P. L. (2021). Historical variability and lifecycles of North Atlantic midlatitude cyclones originating in the tropics. *Journal of Geophysical Research: Atmospheres*, *126*, e2020JD033924. https://doi.org/10.1029/2020JD033924

Received 21 SEP 2020
Accepted 24 FEB 2021

This article has an extended publication history. It was originally submitted to Geophysical Research Letters on December 2nd, 2019 then transferred to Journal of Geophysical Research: Atmospheres on September 18, 2020.

Abstract North Atlantic tropical and post-tropical cyclones impact midlatitude regions, but the inhomogeneous observational record of the latter stages of tropical cyclones precludes many climatological analyses. The frequency of tropical-origin storms basin-wide is projected to increase under anthropogenic climate change, so establishing confidence in our knowledge of their historical variability and lifecycles—against which climate model simulations may be evaluated—is important. We used a Lagrangian feature-tracking algorithm to identify tropical cyclones that impacted Northeast North America and Europe in seven global reanalysis data sets, distinguishing systems that retained warm-core structures or underwent warm seclusion from those that underwent extratropical transition, acquiring cold-core, frontal structures. Over the last four decades, ~25% and ~10% of tropical-origin cyclones made landfall across Northeast North America and Europe, respectively, as warm-core systems, with, on average, higher wind speeds than cold-core systems. Historical warm-core and cold-core landfalls also exhibit distinct tracks, likely responding to differing steering flow and midlatitude conditions.

Plain Language Summary Tropical cyclones and their impacts are not confined to the tropics. In the North Atlantic, the historical record of observed tropical cyclones is probably better than anywhere else, yet even this record is unreliable for storms that originate in the tropics and migrate to the midlatitudes, a particular danger to North American and European coastal regions. Operational collection of pre-satellite aerial and ship-based observations has changed over time, and the record of storm landfalls outside the United States is incomplete. These data issues matter because the frequency of tropical-origin storms across the midlatitudes is expected to increase under anthropogenic climate change, and the basis of any assessment of future risk must be a robust historical understanding. We therefore turned to reanalyses (gridded climate data sets) and an objective storm-tracking algorithm to identify tropical cyclones that impacted two regions: Northeast North America and Europe. We examined the lifecycles of these storms and their nature and intensity at landfall. Over the last four decades, approximately one in four landfalls over Northeast North America exhibited tropical-cyclone characteristics, and such storms are associated with high wind speeds, posing a greater risk. For Europe, that number is one in 10, a surprisingly high proportion. How this may change in future will affect populous regions on both sides of the North Atlantic.

1. Introduction

Tropical and post-tropical cyclones are an important natural hazard across the midlatitude North Atlantic (Bieli et al., 2019; Evans et al., 2017; Jones et al., 2003; Keller et al., 2019). The poleward propagation of tropical cyclones across this basin as well as the occurrence of extratropical transition expose the Northeast United States, maritime eastern Canada, and Europe to hurricane-force wind speeds and extreme precipitation. These are populous and economically important regions, where risks to life and infrastructure are high. For instance, Hurricane Sandy (October 22–29, 2012)—the fourth costliest North Atlantic hurricane yet recorded—caused devastation across the Northeast United States and eastern Canada (Blake et al., 2013). Ex-hurricane Ophelia (October 9–15, 2017) caused severe wind damage across Ireland, the United Kingdom, and Scandinavia (Stewart, 2018). These systems possessed tropical-cyclone-like structural characteristics and intensities at or near landfall, and significant human and economic impacts occurred during their post-tropical stages.

Poleward shifts in the locations of tropical cyclone cyclogenesis (Daloz & Camargo, 2018) and lifetime-maximum intensity (Kossin et al., 2014) have been observed globally, both of which imply an increased risk of tropical-cyclone-related hazards beyond the tropics. Recent studies (Sharmila & Walsh, 2018; Studholme & Gulev, 2018) linked these poleward trends to a poleward expansion of the northern terminus of the tropical-mean Hadley circulation, spreading environmental conditions conducive to tropical cyclones poleward. The frequency of extratropical transition events may respond to these poleward trends and to changes in the midlatitude environment (Evans et al., 2017). An important question is how the risk of landfalling tropical-origin cyclones may change across the midlatitudes in future. Using a global ∼25-km-resolution atmosphere model with prescribed sea-surface temperature forcing, Haarsma et al. (2013) projected an increased frequency of hurricane-intensity storms impacting Europe by the end of the 21st century. Tropical cyclones are likely to experience less dissipation during their poleward propagation under future conditions (a consequence of higher sea-surface temperature and an expanded potential cyclogenesis region), facilitating reintensification in the midlatitudes by merging with baroclinic waves (Haarsma et al., 2013). Moreover, modeling of Hurricane Irene's (2011) extratropical transition revealed that more intense precipitation, stronger near-surface wind speeds, and greater northward propagation are expected in a warmer climate (Jung & Lackmann, 2019). However, the present lack of multimodel studies limits our confidence in projected post-tropical cyclone activity in a warmer climate. To assess recent projections (Haarsma et al., 2013; Liu et al., 2017) and state-of-the-art future simulations from high-resolution, tropical-cyclone-permitting global climate models (e.g., Haarsma et al., 2016; Roberts et al., 2020a), a consensus climatological perspective is required for the historical period.

Recent studies on the evolution of tropical cyclones in the midlatitudes have focused on extratropical transition events, both case studies (e.g., Laurila et al., 2019) and climatological studies of reanalysis (e.g., Bieli et al., 2019) and climate model (e.g., Bieli et al., 2020; Zarzycki et al., 2017) data. Based on European Centre for Medium-Range Weather Forecasts' operational analysis data, 47–61% of Northern Hemisphere tropical cyclones between 2008 and 2012 underwent extratropical transition (Studholme et al., 2015), although estimates are sensitive to the criteria used to identify extratropical transition. National Hurricane Center Hurricane Database version 2 (HURDAT2) best-track data (Landsea & Franklin, 2013), the reference tropical cyclone data set for the North Atlantic, contain well-documented inhomogeneities (Schreck et al., 2014), introduced by various changes in observing capability and practices and historical events (Vecchi & Knutson, 2008), and are subject to ongoing quality-control (Landsea & Franklin, 2013) and revision based primarily on Comprehensive Ocean and Atmosphere Data Set observations (Delgado et al., 2018; Hagen et al., 2012). The HURDAT2 data set is limited by missing storms and intensity underestimation (Vecchi & Knutson, 2008, 2011), particularly in the central and eastern North Atlantic during the pre-satellite era (i.e., pre-1966; conservatively pre-1979), and non-US landfalls are flagged in HURDAT2 only since 1991. Revisions of HURDAT2 over the period that includes aircraft-based reconnaissance observations (post-1944) reveals approximately two missing systems per year, particularly over the central and eastern North Atlantic (Delgado et al., 2018; Hagen et al., 2012). Other recent estimates of the number of cyclones during the pre-satellite period missing from HURDAT2 range from one (approximately category 1) cyclone per year, based on a large ensemble of tropical-cyclone-permitting global model simulations (Mei et al., 2019), to four cyclones per year prior to aircraft reconnaissance (Vecchi & Knutson, 2011). Historically, tropical cyclones recorded in HURDAT2 have not been observed operationally following extratropical transition to cyclolysis, and those which have are affected by uncertainty arising from operational assessment of satellite imagery and information (Delgado et al., 2018). Therefore, the post-tropical stages of storms in HURDAT2 are less well-recorded, effectively precluding many climatological analyses and necessitating the use of reanalysis data sets that provide independent global climate realizations—constrained by observations—and a larger sample from which to quantify historical variability of tropical-origin cyclones in the midlatitudes. Crucially, objective determination of entire cyclone lifecycles—from precursor to post-tropical stage to cyclolysis—is possible with reanalyses (Hodges et al., 2017).

Extratropical transition refers to the transformation of an axisymmetric, warm-core tropical cyclone to an asymmetric, cold-core and vertically tilted extratropical cyclone (Evans et al., 2017; Hart & Evans, 2001; Zarzycki et al., 2017). In the North Atlantic, extratropical transition is typically initiated by loss of thermal axisymmetry with subsequent cold-core development (Studholme et al., 2015), but cold-core development occurs first in approximately one-third of cases (Bieli et al., 2019), or both changes may occur simultaneously.

Table 1
Reanalyses Evaluated in This Study

	Analysis period	Analysis grid	Model resolution (grid spacing)	Data assimilation	Sample size
ERAI	1979–2017	512 × 256	TL255L60 (80 km)	4D-Var.	137, 59
ERA5	1979–2018	1,140 × 721	T639L137 (33 km)	4D-Var.	269, 104
JRA25	1979–2013	288 × 145	T106L40 (120 km)	3D-Var.	129, 48
JRA55	1958–2017	288 × 145	TL319L60 (55 km)	4D-Var.	246, 97
MERRA	1979–2015	540 × 361	1/2 × 2/3 L72 (55 km)	3D-Var. + GSI + IAU	111, 51
MERRA2	1980–2016	576 × 361	Cubed sphere (50 km)	3D-Var. + GSI + IAU	128, 60
NCEP	1979–2016	720 × 361	T382L64 (38 km)	3D-Var. + GSI	138, 63

Note. Nominal resolution at 50°N in units of km is given in brackets. 3(4)D-Var, 3(4)D variational data assimilation; GSI, Grid-point Statistical Interpolation; IAU, Incremental Analysis Update. Analysis grid is the horizontal grid on which tracking was performed. Tropical cyclone representation in these reanalyses (except the ERA5 reanalysis) was evaluated by Hodges et al. (2017), with consistent cyclone tracking and identification as in Section 2. The total tropical-origin cyclone sample size for each landfall domain is given as n_{NENAm}, n_{Europe}.

An early assessment of observed historical post-tropical cyclone variability (Hart & Evans, 2001) revealed that then-available pressure observations were insufficient to estimate post-tropical changes in central pressure in approximately two-thirds of cases. For the remaining third, many observational estimates disagreed with estimates from coarse-resolution (2.5°) ERA-15 reanalysis data, precluding climatological characterization of post-transition cyclone evolution.

Bieli et al. (2019) quantified historical interannual variability of extratropical-transitioning systems in two reanalyses, based on tracks truncated to resemble best-track data, revealing 3–4 transitioned storm landfalls per year in the North Atlantic basin. Identifying post-tropical cyclones only as instances of extratropical transition is sensitive to how well vertical tropical-cyclone structure is represented in a given reanalysis, resulting in missed identifications compared with observed systems. It also requires the use of arbitrary thresholds to distinguish warm-core from cold-core structures and frontal from axisymmetric systems, and necessarily excludes nontransitioning tropical cyclones from analysis. To mitigate these limitations, we combined a well-established cyclone-tracking methodology and two complementary sampling strategies to capture all cyclones originating in the tropics that propagate to midlatitudes—both warm-core and cold-core systems. Our overarching goal is to establish a reanalyses-based climatology to inform contemporary midlatitude storm risk assessments and provide a robust reference against which to evaluate global climate model simulations. We first identify and track North Atlantic tropical cyclones objectively in seven global reanalysis data sets, then perform both objective, phase-space-based identification of extratropical transition and warm seclusion, as per previous studies, and spatial sampling to identify all tropical-origin systems that made landfall in Northeast North America or Europe. The latter captures all post-tropical lifecycles, including extratropical transition and warm seclusion, allowing us to examine the historical variability of tropical-origin cyclone occurrence as well as their structural evolution, intensity, tracks, and landfall characteristics. The rest of this paper is structured as follows. Section 2 describes the reanalysis and best-track data sets used in this study; the tropical-cyclone identification and tracking methodology; and methodologies used to perform cyclone subsampling, cyclone phase-space analysis, and cyclone lifecycle analysis. Results are presented in Section 3 and conclusions in Section 4.

2. Methods

2.1. Data

Our systematic climatological study is based on data over the period 1979–2018 from seven widely used reanalyses (Table 1), which combine a weather forecast model with continuous assimilation of observational data to construct a global representation of historical atmospheric variability. We used the European Centre for Medium-Range Weather Forecasts' Interim Reanalysis (ERAI; Dee et al., 2011) and Fifth Reanalysis (ERA5; Hersbach et al., 2020); the Japanese 25-year Reanalysis (JRA25; Onogi et al., 2007) and

55-year Reanalysis (JRA55; Kobayashi et al., 2015); the National Aeronautics and Space Administration's Modern-Era Retrospective Analysis for Research and Applications (MERRA; Rienecker et al., 2011) and subsequent version 2 (MERRA2; Molod et al., 2015); and the combined National Centre for Environmental Prediction Climate Forecast System Reanalysis and Climate Forecast System version 2 data set (NCEP; Saha et al., 2014), which is the sole fully coupled (atmosphere, ocean, land surface, and sea ice) reanalysis in this study. In JRA25, JRA55, and NCEP, the use of "bogussing" improves the representation of tropical cyclones by adjusting the simulated vortex location to its observed location prior to the assimilation of storm circulation observations. In JRA25, bogus data are synthetic wind profiles (Onogi et al., 2007). In JRA55, bogus wind observations are taken from the Japanese Meteorological Agency's operational analysis (Kobayashi et al., 2015). In NCEP, historical storm report wind estimates are bogussed (Saha et al., 2014). The dense coverage of meteorological observations, particularly temperature and pressure, across the North Atlantic reduce reanalysis uncertainty compared with other ocean basins. Reanalyses provide the only long-term and observationally constrained global data sets upon which analysis of the structural evolution of historical tropical cyclones may be based. We include HURDAT2 data (Landsea & Franklin, 2013) for comparison but, due to its limitations in examining post-tropical cyclones, not as a definitive reference against which to evaluate the reanalyses' performance.

2.2. Lagrangian Tropical-Cyclone Tracking

To identify and track the evolution of tropical cyclones consistently across seven reanalysis data sets in this study, we used the objective Lagrangian feature-tracking algorithm—*TRACK*—of Hodges (1995), a well-established tool for identifying tropical cyclones in reanalyses (Hodges et al., 2017). The *TRACK* algorithm was applied to six-hourly, vertically averaged relative vorticity, computed from zonal and meridional wind fields at the 850, 700, and 600 hPa isobaric levels. Vertically averaged vorticity data were then spectrally filtered to T63 resolution to remove small-scale noise (total wavenumbers >63) and planetary scales (total wavenumbers 0–5). Vorticity maxima exceeding 0.5×10^{-5} s^{-1} were identified and initialized into tracks using a nearest-neighbor approach and subsequently refined by minimizing a cost function for track smoothness, subject to adaptive constraints on track displacement and smoothness (Hodges, 1995, 1999). Following tracking, cyclone-centered sampling of meteorological fields along cyclone tracks was performed to detect warm-core structures and measure cyclone intensities, following Hodges et al. (2017). For warm-core identification, the T63-truncated (i.e., no removal of planetary scales) vorticity data at the 850, 700, 600, 500, 400, 300, and 200 hPa levels were added to tracks by recursively searching for a vorticity maximum at each level using the previous level's maximum as the starting point for a steepest-ascent maximization applied to the B-spline-interpolated field. A search radius of 5° was used, centered on each level's maximum. Following Hodges et al. (2017), objective identification of tropical cyclones adhered to the following criteria:

- cyclogenesis equatorward of 30°N
- total cyclone lifetime must exceed 2 days
- T63 relative vorticity at 850 hPa must exceed 6×10^{-5} s^{-1}
- T63 relative vorticity center must exist at each level between 850 and 200 hPa to indicate a coherent vertical structure
- T63 relative vorticity decrease with increasing height between 850 and 200 hPa by at least 6×10^{-5} s^{-1} to indicate the presence of a warm core

The three T63 relative vorticity criteria must also be jointly attained for at least four consecutive time steps (i.e., 1 day) over ocean. Together, these criteria minimize inclusion of spurious short-lived or relatively weak vorticity features.

Further cyclone-centered sampling of meteorological fields was performed. To quantify cyclone intensity, minimum sea-level pressure minima within a radius of 5° and 925-hPa and 10-m wind speed maxima within a radius of 6° of the storm center were sampled from reanalysis fields at their full, nontruncated resolutions (Table 1). All search radii are geodesic. This methodology was documented in greater detail by Hodges et al. (2017) and is consistent with recently published analysis of tropical cyclones in global climate models (e.g., Roberts et al., 2020a). Crucial to our study, vorticity-based tracking and identifying tropical cyclones after tracking yields longer cyclone lifetimes (compared with central-pressure-based algorithms and methodologies where identification criteria are applied as part of the tracking), capturing a storm's

precursor stage and allowing for objective analysis of the evolution of the post-tropical storm stages (Hodges et al., 2017). Despite these advantages, we acknowledge that comparisons with other tracking algorithms in future would be advantageous. Finally, spatial track statistics—track and genesis density—were computed using spherical kernel estimators, following Hodges (1996).

2.3. Spatial Cyclone Subsampling and Landfall Determination

From objectively identified tropical cyclones, we sampled systems that passed within two landfall domains (Figure S1): Northeast North America (land area within 35–60°N, 60–85°W; hereafter "NENAm") and Europe (land area within 36–70°N, 10°W–30°E), representing the north-western and north-eastern margins, respectively, of the observed spatial distribution of tropical cyclone tracks over the North Atlantic. Landfall within these domains was determined objectively: a storm is considered to be landfalling if its center passes within 200 km of the coastline for at least one time step, based on Global Self-consistent Hierarchical High-resolution Geography coastline data (Wessel & Smith, 1996). Our rationale in using this criterion reflects the fact that cyclone winds may be experienced along a coastline before the storm center intersects that coastline. The National Hurricane Center defines the diameter of a storm's "strike circle" as 125 nautical miles (232 km) and defines a "direct hit" to be when the distance between storm center and coastline is less than the storm's radius of maximum wind (if the storm is to the right of the coastline) or two times the radius of maximum wind (if the storm is to the left of the coastline). Our use of 200 km also accounts for any increase in storm size as a cyclone translates poleward. Reducing this to 100 km does not significantly change our results. For consistency, we applied this subsampling criterion to the HURDAT2 data set to avoid relying upon HURDAT2's limited non-US landfall flagging. This spatial sampling captures all tropical-origin cyclones that propagate to each landfall domain and distinguishes separate landfalls for any system which makes landfall in NENAm and subsequently in Europe, and any system which makes landfall more than once within the same landfall domain is considered a single landfalling cyclone.

2.4. Cyclone Phase-Space Analysis

The temporal evolution of cyclone structure is quantifiable by analysis of a cyclone's thermal wind fields (Hart, 2003; Hart & Evans, 2001). The so-called cyclone phase-space analysis involves three parameters: the thermal symmetry of the cyclone (B) and the lower-tropospheric (T_L) and upper-tropospheric cyclone-relative thermal wind (T_U). B is defined as

$$B = h\left(\overline{Z_{600} - Z_{900}}\,|_R \; -\overline{Z_{600} - Z_{900}}\,|_L\right), \tag{1}$$

where $h = 1$ for the Northern Hemisphere, Z_p is geopotential height (m) at isobaric level p (hPa), and the subscripts $_R$ and $_L$ denote the right-hand and left-hand semicircles relative to the cyclone's direction of movement, respectively. Following previous research (Dekker et al., 2018; Hart, 2003), we defined thermal axisymmetry (i.e., nonfrontal structure) as $B < 10$ m and asymmetry (i.e., frontal structure) as $B \geq 10$ m. T_L and T_U are defined as vertical derivatives of the horizontal geopotential height gradient

$$T_L \equiv -\left|V_T^L\right| = \frac{\partial\left(\Delta Z\right)}{\partial \ln p}\Big|_{P_l}^{P_u}, \tag{2}$$

$$T_U \equiv -\left|V_T^U\right| = \frac{\partial\left(\Delta Z\right)}{\partial \ln p}\Big|_{P_l}^{P_u}, \tag{3}$$

where p is pressure and $\Delta Z = Z_{\max} - Z_{\min}$, where $Z_{\max}$ and $Z_{\min}$ are the maximum and minimum geopotential height, respectively, at a given isobaric level within a 5° radius of the cyclone center. Hart (2003) used the slope of the linear regression between ΔZ and ln p over several isobaric levels as the derivative of ΔZ relative to ln p (Equations 2 and 3) to determine the mean ΔZ over the pressure range P_l to P_u—the lower and upper levels, respectively. We used three levels—900, 600, and 300 hPa—for all reanalyses except JRA25, for

which 925, 600, and 300 hPa were used. Our use of three vertical levels is consistent with previous studies (e.g., Bieli et al., 2019, 2020; Liu et al., 2017; Studholme et al., 2015), and is preferred because it will allow for future comparisons with climate model output, where the number of available vertical levels is typically restricted.

Positive T_L or T_U values indicate the presence of a warm core in the upper or lower troposphere; negative values indicate a cold core. A deep warm-core or cold-core structure is identified where T_L and T_U are of the same sign. To separate warm-seclusion cyclones from the identified warm-core systems at landfall, we identified cases where $T_L < 0$ (cold-core development) followed by $T_L > 0$ (warm-core redevelopment), each persisting for at least four consecutive time steps (i.e., 1 day). The use of this 1-day criterion identifies meaningful temporal changes in T_L and avoids counting any spurious high-frequency variability in T_L about zero as multiple core structure changes. Cyclone phase-space parameters are also used to identify extratropical transition, which is defined herein as the occurrence of $B \geq 10$ m and $T_L < 0$ for at least 1 day. Use of these thresholds follows previous studies (e.g., Bieli et al., 2019, 2020; Studholme et al., 2015), but systematic sensitivity analysis would be a useful future contribution.

2.5. Cyclone Lifecycle Analysis

Cyclone structures were classified using the cyclone phase-space parameters at the point of landfall. To construct composite lifecycles, storms for each phase-space category were temporally aligned by their landfall point (i.e., $t = 0$) and composite cyclone-associated maximum 10-m wind speed, v_{max}, and minimum sea-level pressure, p_{min}, time series were computed. In this analysis, a storm may not exist in more than one phase-space category.

3. Results and Discussion

3.1. Spatial Cyclone Statistics

Across the North Atlantic, the spatial pattern of annual-mean track density for all tropical-origin cyclones reaching NENAm is highly consistent between the reanalyses, so we show the multireanalysis-mean field. Track density values close to coastal regions are 2–5 cyclones year^{-1} (Figure 1a). Climatological genesis density maxima are found close to the Florida peninsula, indicating that tropical and post-tropical cyclones that reach the NENAm form close to the United States mainland, and secondary maxima are seen over West Africa at ~10°N, associated with African easterly wave propagation. This highlights the importance of a cyclone-tracking methodology which captures cyclones' precursor stages. While tropical storm genesis over land is rare, precursor genesis (i.e., the early vorticity anomaly), which is captured by reanalyses, may occur over land. For tropical-origin cyclones impacting Europe, the spatial pattern of track density is also comparable between reanalyses, with ~2 cyclones year^{-1} along the midlatitude North Atlantic storm track, reflecting the recurvature and westerly propagation of tropical cyclones (Figure 1b). Climatologically, approximately twice as many tropical-origin storms reach northern Europe than southern Europe. A secondary maximum localized around the Iberian Peninsula, associated with cyclogenesis close to Europe, is seen in some, but not all, reanalyses and is therefore averaged out of the multireanalysis-mean track statistics. We interpret these systems as arising from interaction between African Easterly Waves and equatorial waves (Yang et al., 2018), resulting in cyclone tracks that undergo reduced westward storm translation prior to recurvature. Cyclogenesis regions for NENAm and Europe are generally colocated, except for genesis over the Caribbean basin, which is less important for Europe.

3.2. Interannual Variability and Seasonal Cycle

In this section, we first consider all North Atlantic tropical cyclones undergoing extratropical transition and then separately analyze all tropical cyclones reaching each landfall domain, regardless of whether they undergo extratropical transition.

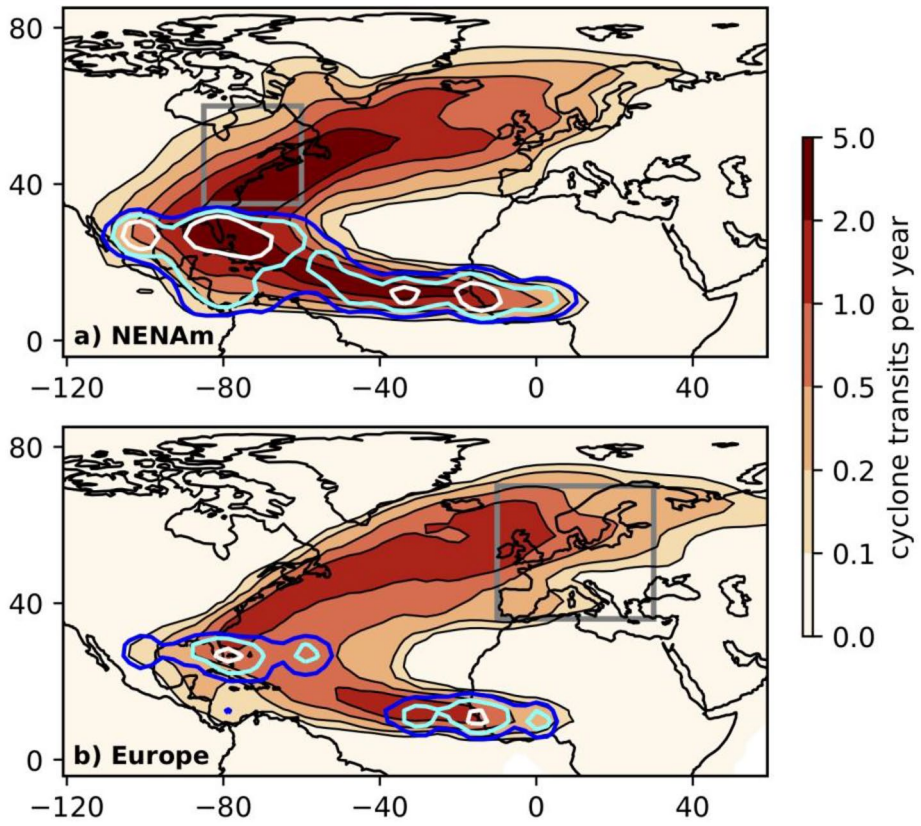

Figure 1. Climatological annual-mean cyclone track (filled contours) and genesis (overlain contours) density derived from all objectively identified cyclones identified during only the years common across all seven reanalyses (1980–2013; see Table 1). Climatologies represent all tropical-origin systems making landfall in (a) NENAm and (b) Europe. Genesis density contours are drawn at 0.01 (blue), 0.05 (cyan), and 0.1 (white). Units are cyclones per month per unit area (within a 5° radial cap centered on storms). Landfall domains are also indicated (gray boxes), which outline the land areas defined in Figure S1. NENAm, Northeast North America.

3.2.1. Basin-Wide Trends in Extratropical Transition

Across the whole North Atlantic basin, four reanalyses show statistically significant positive trends in the number of tropical cyclones undergoing extratropical transition and three show significant positive trends in the percentage of all tropical cyclones which transition (Figure 2). No negative trends are found and only ERA5 exhibits no trend in either variability metric. Interannual variability in both metrics is highly consistent between reanalyses, albeit less so for extratropical transition percentage. Continued positive trends are projected by simulations where sea-surface temperature biases are corrected (Liu et al., 2017). However, Bieli et al. (2019) found no significant trends in ERAI or JRA55 over the North Atlantic, based on a definition of extratropical transition modified to maximize agreement between transition cases identified in these two reanalyses with those inferred from best-track data flags. However, our analysis differs by not focusing on reanalysis storms matched to best-track data. Moreover, such matching of extratropical transition events may introduce uncertainties related to the fact that tropical cyclone interannual variability compares more favorably between reanalyses and best-track data sets when weaker systems are excluded (Hodges et al., 2017). Additionally, we determined a somewhat higher extratropical transition percentage compared with Bieli et al. (2019), which is more in line with Studholme et al. (2015). These differing percentages and apparently contradictory temporal trends highlight the need for a consensus phase-space-based definition of extratropical transition. It should be acknowledged that the representation of tropical cyclones in older reanalyses, particularly MERRA, is comparatively poor (Hodges et al., 2017).

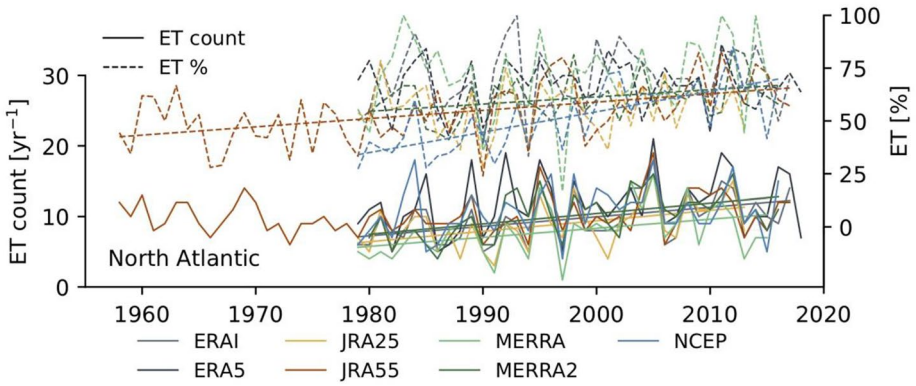

Figure 2. Interannual variability of (solid lines; left-hand *y* axis) extratropical transition events and (dashed lines; right-hand *y* axis) the percentage of tropical cyclones undergoing extratropical transition over the North Atlantic, as diagnosed by a cyclone phase-space-based definition of extratropical transition (see Section 2). Only statistically significant linear trends (i.e., $p < 0.05$) are shown.

3.2.2. Seasonal Cycle and Interannual Variability of Landfalling Tropical-Origin Cyclones

We now consider all tropical-origin cyclones, identified by spatially subsampling tracked tropical cyclones, whether or not extratropical transition occurs. Together, reanalyses capture the observed seasonal cycle of North Atlantic tropical cyclones (Figure 3a). The seasonality of tropical-origin cyclones reaching NENAm and Europe closely follows the overall monthly distribution of North Atlantic tropical cyclones (Figures 3b and 3c), with good interreanalysis agreement on the initiation of cyclone activity in July, peaking in September, and the cessation of activity in November. These seasonal timings in reanalyses are in good agreement with HURDAT2 data. Moreover, the magnitude of the seasonal peak in September for NENAm is well matched between reanalyses and HURDAT2 (Figure 3b). For Europe, however, reanalyses overestimate this peak compared with HURDAT2 (Figure 3c). Known issues and limitations in best-track data, several of which affect the central and eastern North Atlantic, suggest that the frequency of tropical-origin storms impacting Europe is likely underestimated in HURDAT2. Multireanalysis-mean peak values are ~2 and ~0.7 cyclones month^{-1} for NENAm and Europe, respectively. For Europe, a secondary, earlier peak during May-June is observed in ERA5, but this is less apparent in the other data sets. At the climatological peak of the North Atlantic tropical cyclone season in September, reanalyses show that between 30% and 50% of tropical cyclones reach NENAm (Figure 3d), consistent with Zarzycki et al. (2017), and between 10% and 20% reach Europe (Figure 3e), but higher percentages are seen during late winter and spring. For NENAm, high percentage values in reanalyses during January and February are similar to HURDAT2 (Figure 3d), but a caveat here is that there are few early year tropical-origin systems in the best-track data. These high early year percentages likely reflect strong interactions between the tropical Atlantic and midlatitude storm tracks during the equinoctial seasons. Together with similar early year detections in previous analysis of ERAI and NCEP (Zarzycki et al., 2017), these results highlight how objective tropical-cyclone tracking and identification yields systems during late boreal winter that seldom occur in best-track data.

Regarding the interannual variability of cyclones reaching NENAm and Europe, no significant trends are found in either the total count of tropical-origin cyclones since 1979 (1958 for JRA55; 1980 for MERRA2), although counts are somewhat higher during the satellite era, and pronounced interannual variability exists (Figure 4). Climatologically, NENAm and Europe have experienced four and two tropical-origin cyclone landfalls per year, respectively. This highlights that, while landfalls at near-hurricane intensity are historically rare, landfalling tropical-origin storms are a climatological feature across the midlatitude North Atlantic. Interannual variability in annual tropical-origin cyclone count is significantly, positively correlated between reanalyses (and between reanalyses and HURDAT2) over the common period of 1980–2013, with Spearman's ρ coefficients (nonparametric rank correlations) between ~0.5 and ~0.8 ($p \leq 0.01$), with generally stronger correlations for NENAm compared with Europe (Figure 5). That reanalysis-HURDAT2 ρ values are weaker for Europe than for NENAm is consistent with where we expect best-track data to be less reliable. Key HURDAT2 limitations—namely, missing storms over the central and eastern North Atlantic

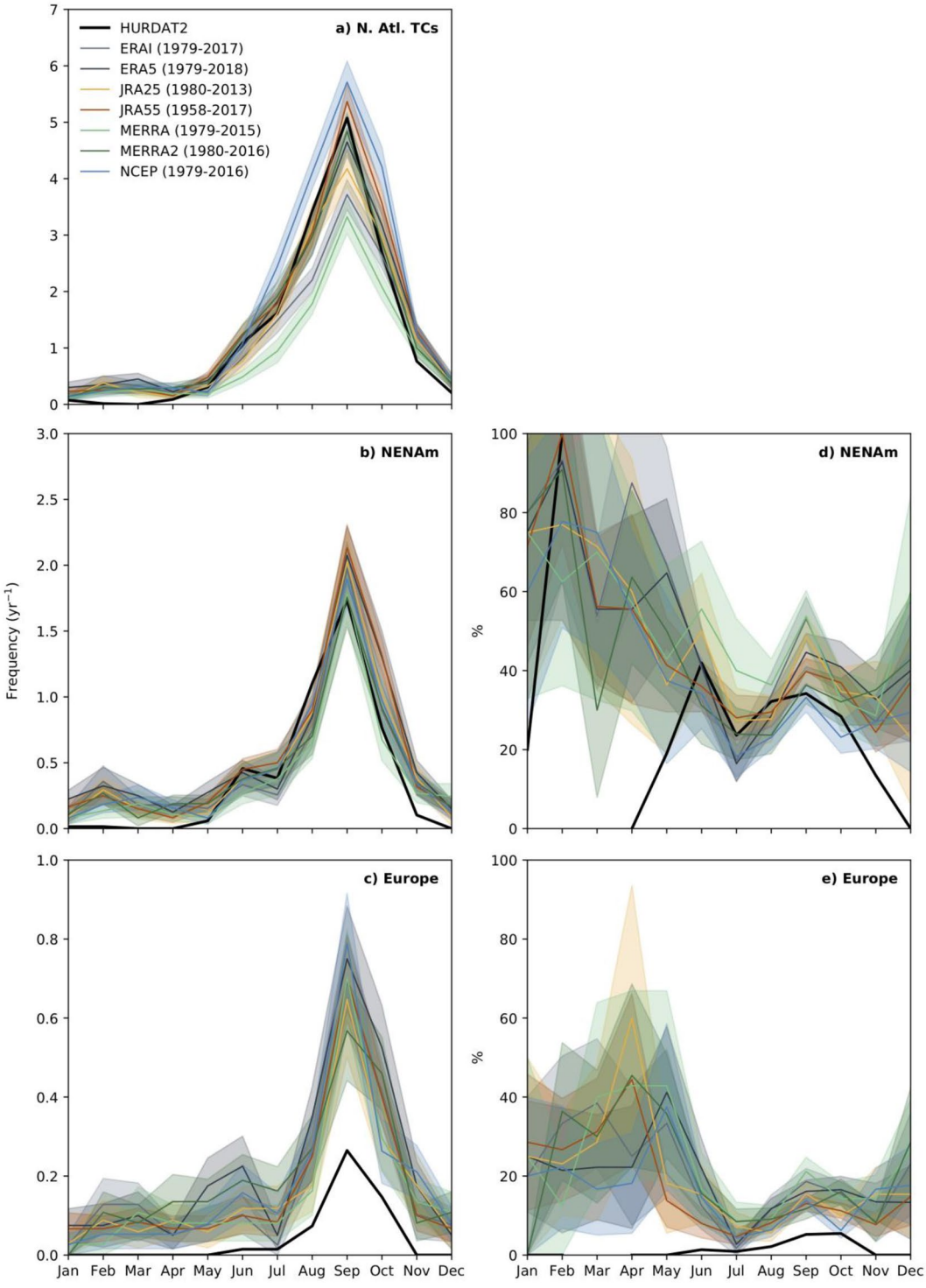

Figure 3. Seasonal cycle of the number of (a) North Atlantic tropical cyclones and of the number of landfalling tropical-origin cyclones reaching (b, d) NENAm and (c, e) Europe, expressed as (left-hand panels) an annual-mean count and (right-hand panels) a percentage of all tropical cyclones, both computed for all available years for each reanalysis. Cyclones were binned by the month of occurrence of lifetime-maximum intensity (lowest p_{min}). No systems making landfall over NENAm or Europe were identified in HURDAT2 during March. Shading shows 1 standard deviation of interannual variability. Note the various *y* axis scales. NENAm, Northeast North America.

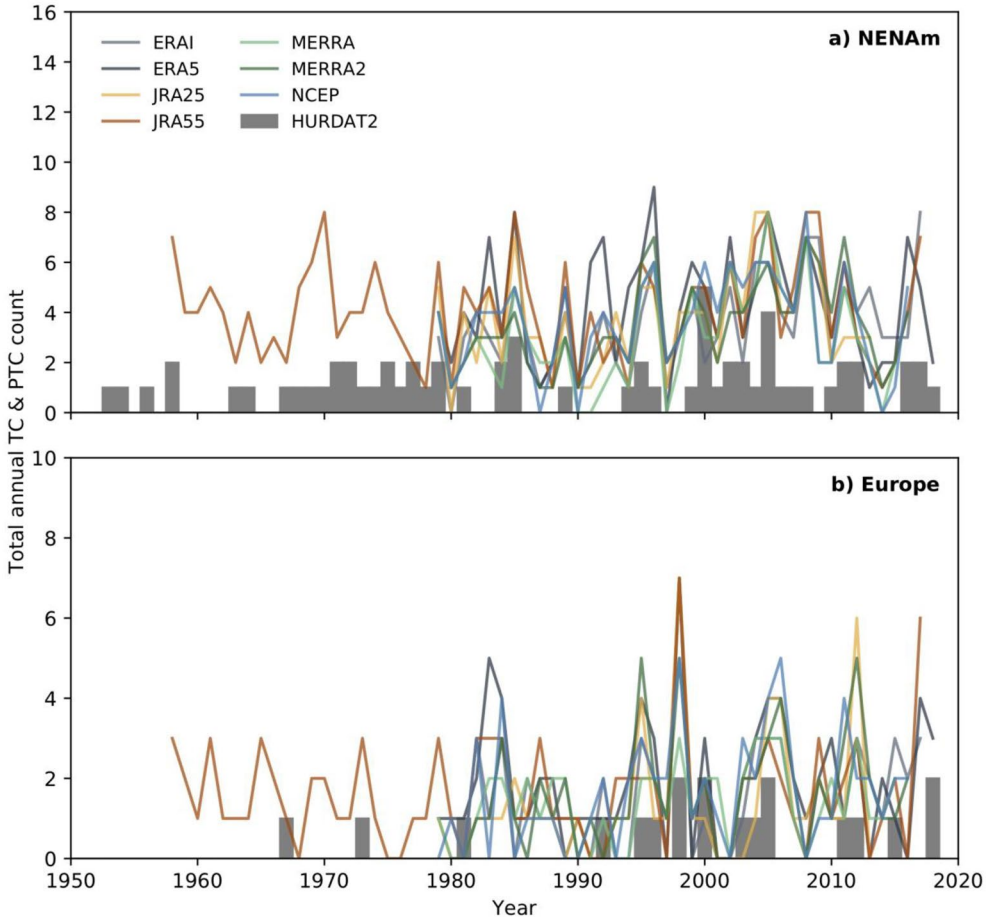

Figure 4. Interannual variability in the number of tropical-origin cyclones reaching (a) NENAm and (b) Europe in HURDAT2 (gray bars) and reanalyses (colored lines). Note the different *y* axis scales. NENAm, Northeast North America.

and less well observed (or unobserved) post-tropical storm stages (Delgado et al., 2018; Hagen et al., 2012)—can explain reduced interannual correlation between best-track data and reanalyses. The somewhat weaker interreanalysis ρ values for Europe compared with NENAm likely reflect the fact that both the midlatitude environment must be conducive to either sustain tropical cyclones after recurvature or allow extratropical transition, and that the steering flow must be sufficient for these systems to reach Europe. How these mid-latitude conditions control downstream variability of tropical-origin cyclones and how such conditions are represented by both reanalyses and global climate models are important subjects for further studies.

The intermittency of non-US landfall information prior to 1991 limits the HURDAT2 record of European tropical-origin cyclone activity, so quantifying interreanalysis agreement is important. For both landfall domains, the interreanalysis range in historical year-to-year counts of tropical-origin cyclones is most likely explained by the substantive historical changes in observational capability and the assimilation of observational data as well as the different forecast models used to construct these reanalyses (Table 1). Interreanalysis agreement is generally lower during the early 1980s and JRA55 does not match HURDAT2 well during the pre-satellite period (1958–1979) for either landfall domain (Figure 4), highlighting the impact of observational limitations. The forthcoming extension of ERA5 back to 1950 (Hersbach et al., 2020) will provide another pre-satellite record, but climate model simulations can provide complementary data sets with which to investigate interannual variability.

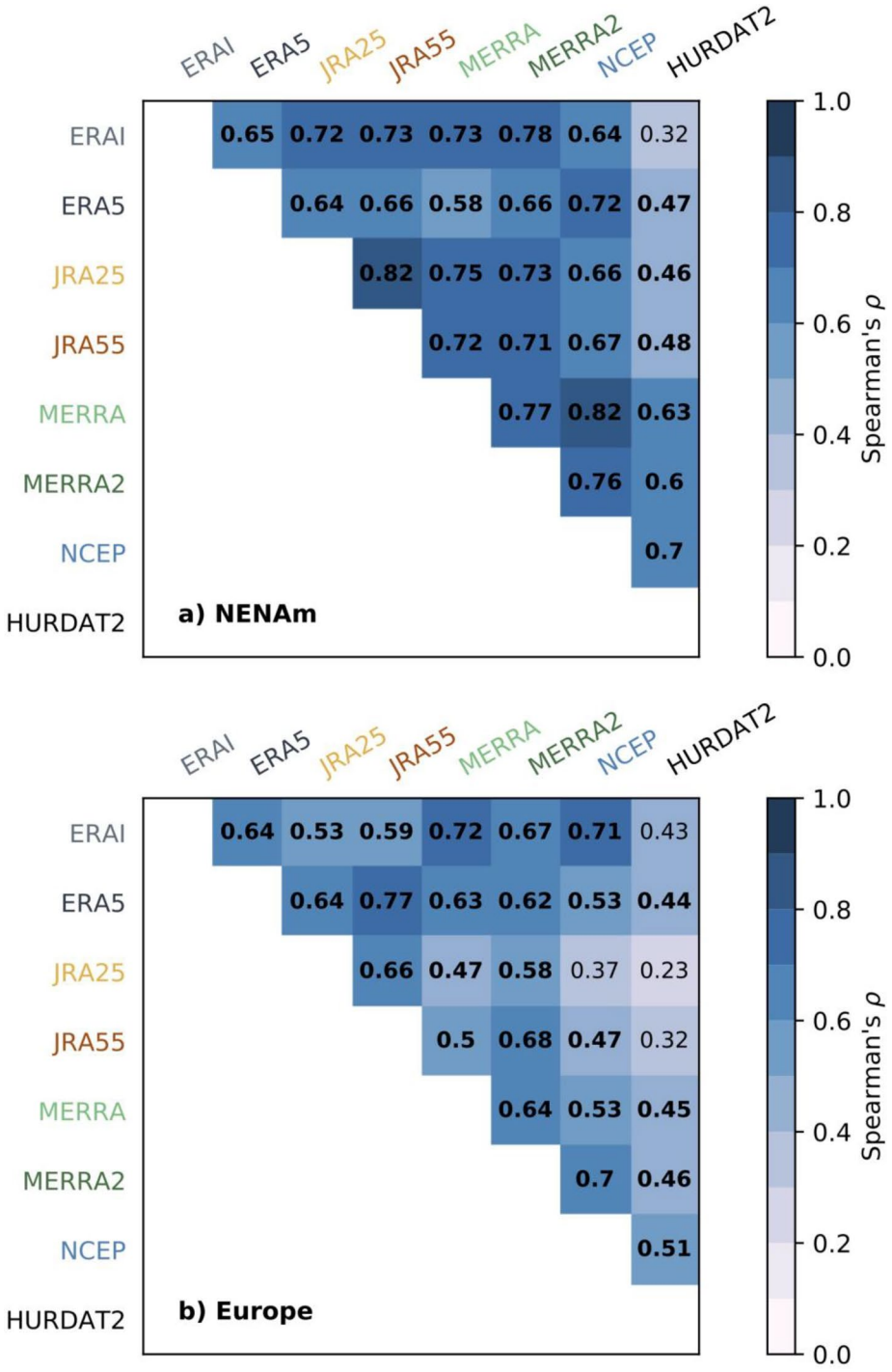

Figure 5. Spearman's coefficients (ρ) for interreanalysis and reanlaysis-HURDAT2 correlations with respect to interannual variability in all tropical-origin cyclones reaching (a) NENAm and (b) Europe. Correlations were performed for the common period 1980–2013. Significant correlations (i.e., $p \leq 0.01$) are indicated by bold type. NENAm, Northeast North America.

3.3. Cyclone Intensity

The probability density of v_{max} (poleward of 30°N) for tropical and post-tropical cyclones reaching each landfall domain exhibits a distribution spanning ~5–40 m s^{-1} (or 960–1,000 hPa in p_{min}—see Figure S2) in the reanalyses (Figure 6). Cyclone v_{max} is underestimated across all reanalyses compared with best-track

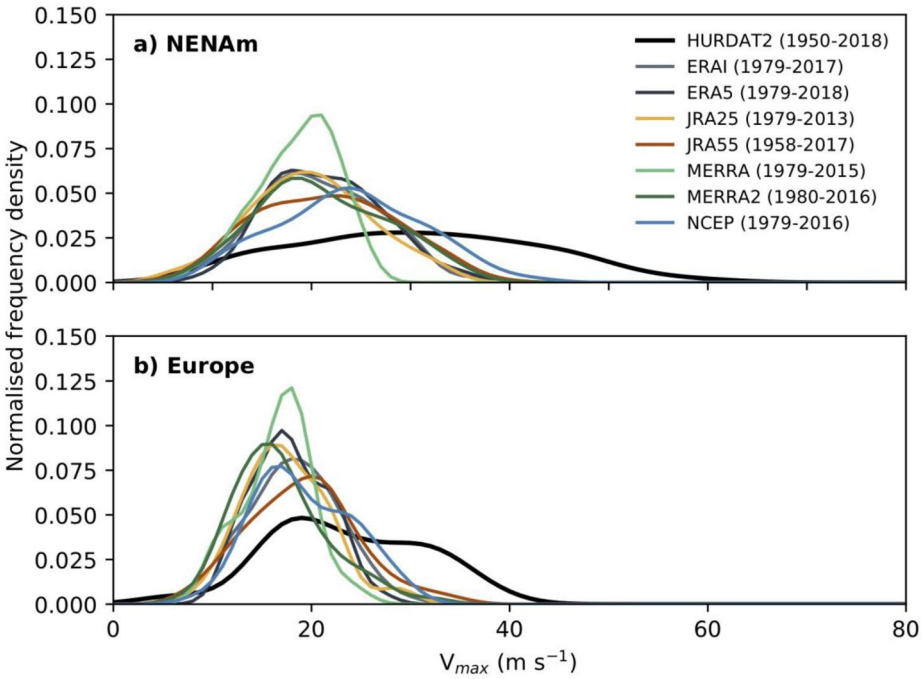

Figure 6. Probability density functions of lifetime-maximum v_{max}, computed by kernel density estimation for all landfalling cyclones reaching (a) NENAm and (b) Europe for all available years for each reanalysis. NENAm, Northeast North America.

estimates, particularly by MERRA (Figure 6), although we caution that HURDAT2 intensity estimates are less reliable for transitioning systems (Velden et al., 2006). The intensity discrepancy between reanalyses and HURDAT2 is primarily explained by the relatively low horizontal atmospheric resolutions of the reanalyses (see Table 1), which cannot properly represent hurricane-strength systems (Hodges et al., 2017; Murakami, 2014; Schenkel & Hart, 2012). Additionally, comparatively weak systems are likely to be missing from the pre-satellite HURDAT2 record (Hagen et al., 2012), potentially skewing the best-track distributions. Interreanalysis differences are apparent, with JRA55 and NCEP exhibiting somewhat higher probabilities of stronger systems. In JRA55, however, tropical-cyclone wind profiles are assimilated; this reanalysis is therefore less independent from best-track estimates during cyclones' tropical lifetime stages, although the impact of this is minimized by considering only data poleward of 30°N.

3.4. Cyclone Structure and its Relationship With Intensity

We now focus on the cyclone phase-space properties of tropical and post-tropical cyclones affecting NENAm and Europe, focusing on the structural evolution of cyclones prior to and following landfall.

The proportion of each phase-space structural type, categorized at landfall, is highly consistent across all reanalyses (Figure 7). For NENAm, ~40% of the total tropical and post-tropical cyclones identified in this study exhibit warm-core characteristics ("sym_WC" and "asym_WC"), of which approximately one-third made landfall as an axisymmetric tropical cyclone (Figure 7a), with approximately equal proportions of shallow and deep warm-core structures (Figure 7b). Of those that underwent extratropical transition ("asym_CC"), most evolved a deep cold core as well as thermal asymmetry (Figures 7a and 7b). For Europe, ~70% of landfalling tropical-origin cyclones underwent extratropical transition, but ~15% were warm-core landfalls (Figures 7c and 7d). Subsampling the 50 (arbitrary) most intense cyclones within each reanalysis reveals an increase of ~5% in the proportion of warm-core landfalls over NENAm and a similar decrease in the proportion of cold-core landfalls (Figure S3), which is again consistent across all reanalyses, but this is largely within historical interannual variability. Finally, the shallow cold-core category implies a lower-tropospheric cold-core and upper-tropospheric warm core; these systems are not detected in all reanalyses and are therefore largely disregarded in this discussion.

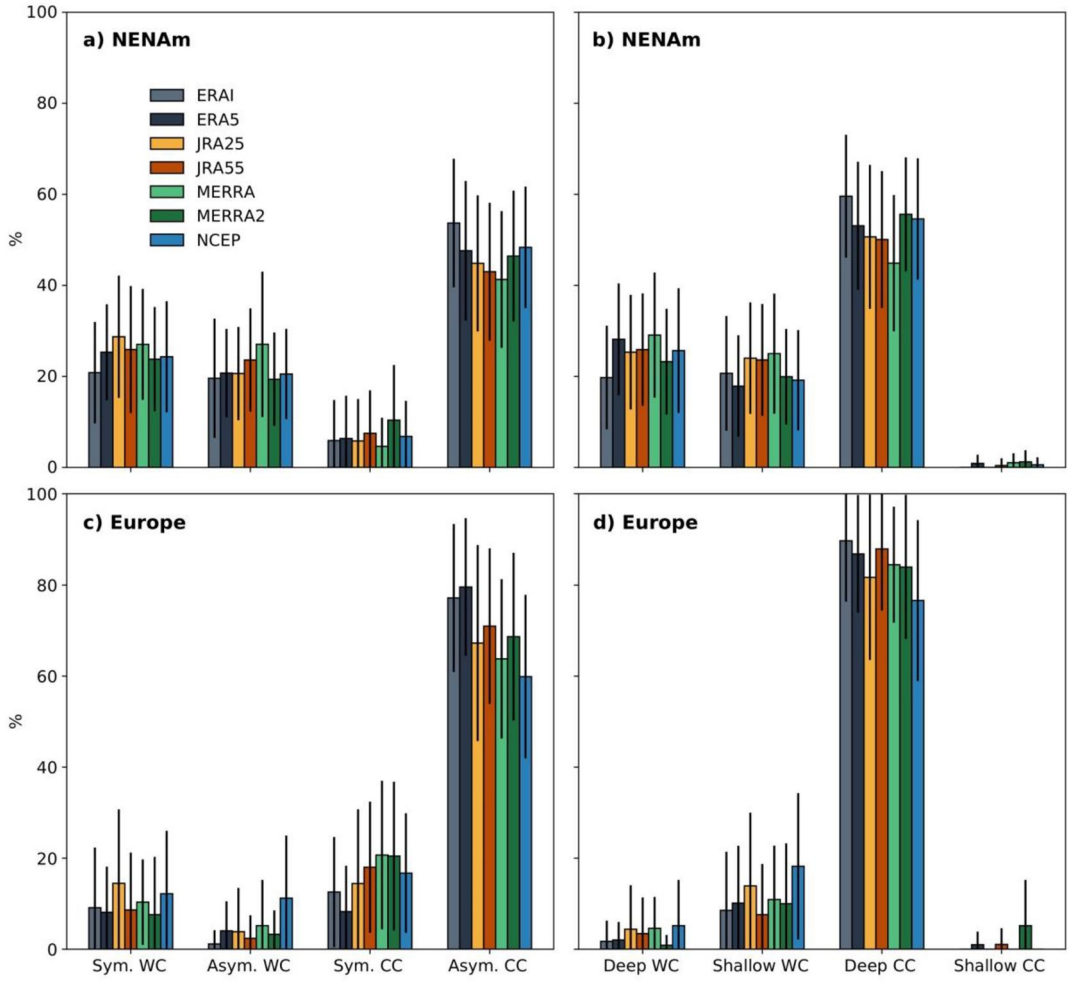

Figure 7. Tropical-origin cyclone structural characteristics at landfall. Vertical core structure was characterized by cyclone phase-space parameter values at landfall for (a, b) NENAm and (c, d) Europe. Vertical error bars show 1 standard deviation of interannual variability. Following Hart (2003), cyclone phase-space categories are shallow (lower-tropospheric) or deep (lower-tropospheric and upper-tropospheric) warm core ("WC") or cold core ("CC") and either symmetrical (i.e., nonfrontal; "Sym.") or asymmetrical (i.e., frontal; "Asym."). NENAm, Northeast North America.

To examine the link between tropical-origin cyclone structure and the potential for severe storm impacts, we computed landfall-centered composite cyclone intensity (measured by p_{min} and v_{max}) time series (Figure 8). By categorizing tropical-origin cyclones according to their phase-space structure at the point of landfall, consistent behavior between the reanalyses is found. For both landfall domains, the most intense systems at landfall exhibit a hybrid structure: tropical warm core and thermal asymmetry ("asym_WC"), the latter indicating the existence of an additional baroclinic energy source (Figures 8a, 8b and 8d, 8e), or else are warm-seclusion systems. The temporal intensity evolution of such systems is largely indistinguishable from warm-seclusion cyclones, which is largely due to the 1-day criterion we employed in identifying seclusion to exclude spurious, short-lived changes in cyclone phase-space parameters (see Section 2). Cyclones that retained both their warm core and thermal axisymmetry—making landfall as a tropical cyclone—are almost as intense at landfall (Figures 8a, 8b and 8d, 8e). For Europe, warm-core landfalls exhibit their deepest p_{min} ~2 days after landfall (Figure 8d), but peak v_{max} occurs ~1 day after landfall (Figure 8e). Clearly, a warm-core structure at or near landfall is associated with greater near-surface hazards compared with cold-core landfalls. The weakest systems for both landfall domains exhibit a hybrid structure comprised of tropical axisymmetry and a cold core ("sym_CC"). These results are consistent across reanalyses and apply to both landfall domains, illustrating the value of spatial sampling in studies of post-tropical cyclones.

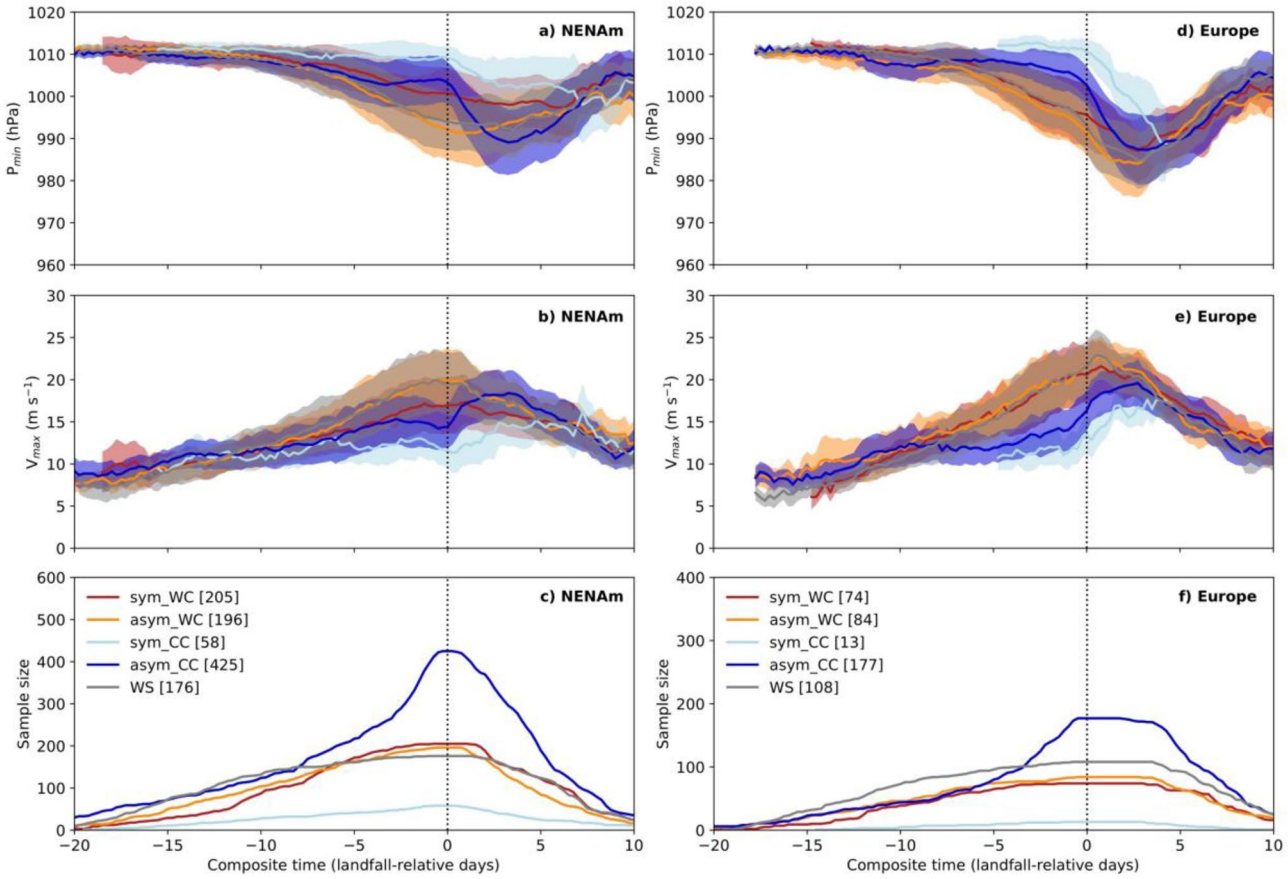

Figure 8. Composite tropical-origin cyclone lifecycle intensity evolution, where intensity is measured by p_{min} (hPa) and v_{max} (m s^{-1}), categorized by cyclone phase-space parameter values at the point of landfall over (a–c) NENAm and (d–f) Europe. Composites are averaged for all cyclones objectively identified across all seven reanalyses. Cyclone lifecycles are landfall-centered (i.e., landfall is indicated by composite day = 0; vertical dashed line) and negative (positive) values denote before (after) landfall. Following Hart (2003), cyclone phase-space categories are either warm ("WC") or cold core ("CC") and either symmetrical (i.e., nonfrontal; "sym") or asymmetrical (i.e., frontal; "asym"). "WS" denotes warm-seclusion systems. Shading shows one standard deviation. To homogenize sampling of pre-landfall and post-landfall intensity evolution, averaging was performed at every landfall-centered time step for which the number of cyclones exceeds 10. The sampling distribution for each composite is given as a function of composite time (c, f). NENAm, Northeast North America.

Tropical cyclones that underwent extratropical transition ("asym_CC") made landfall with lower v_{max} and higher p_{min} than warm-core landfalls (Figures 8a, 8b and 8d, 8e). This typical extratropical-transition lifecycle (Dekker et al., 2018; Hart & Evans, 2001) is the most common among landfalling tropical-origin cyclones (Figures 8c and 8f). For both NENAm and Europe, transitioned, cold-core systems reach their lowest p_{min} and peak v_{max} after landfall (Figures 8a, 8b and 8d, 8e), indicating their maturation as an extratropical cyclone. The composite time series show that such systems' secondary intensification, on average, exceeds their previous peak intensity as a tropical cyclone (Figures 8a, 8b and 8d, 8e), which is important in understanding the associated storm hazards.

3.5. Cyclone Tracks

Finally, we constructed composite cyclone tracks, categorized by core structure at landfall, for both NENAm and Europe (Figure 9) and infer the prevailing steering conditions from each composite track. For NENAm, cyclones making landfall with warm-core structures ("sym_WC," "asym_WC," and "WS") recurve earlier (i.e., at a more eastern longitude) than those reaching the domain with cold-core structures, which, on average, begin to recurve in the vicinity of the Florida peninsula (Figure 9a). This result is consistent with Dekker et al. (2018), except that our composite tracks converge as they enter westerly midlatitude flow. The warm-core composite tracks indicate that these systems do not propagate far over land. For Europe,

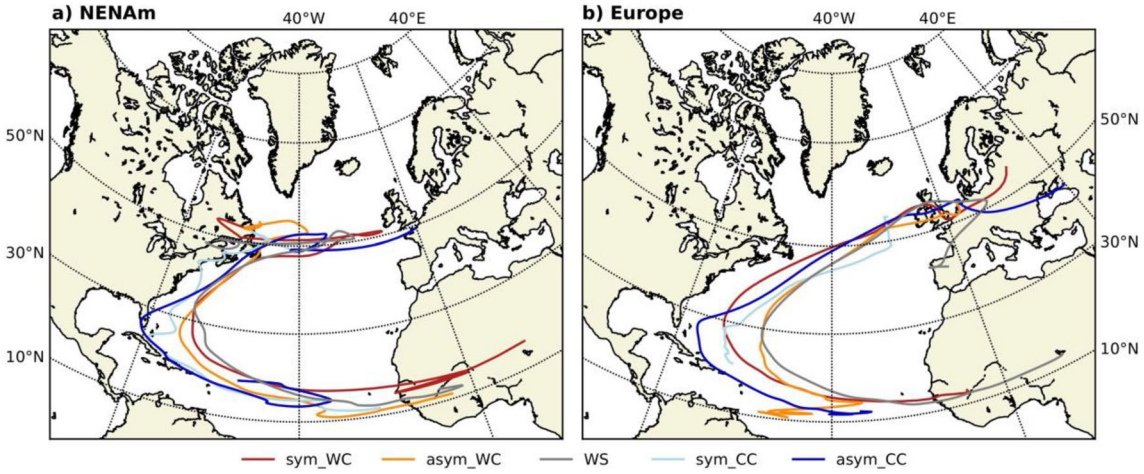

Figure 9. Multireanalysis-mean and phase-space-categorized composite tracks for (a) NENAm and (b) Europe. Composite longitude and latitude positions were computed only where the number of cyclones exceeds 10 and the resultant mean tracks for each phase-space category were smoothed using a cubic spline. Track colors denote landfall core structure for each respective landfall domain (corresponding to Figure 8). NENAm, Northeast North America.

all phase-space categories recurve earlier than those reaching NENAm (Figure 9b), again with warm-core systems recurving earlier than the "asym_CC" track. The tracks converge and overlay one another east of ~40°W, resulting in warm-core and cold-core landfalls over Western Europe at ~55°N (Figure 9b). This highlights the importance of the midlatitude westerly flow in determining downstream cyclone evolution, although variability in the North Atlantic subtropical anticyclone plays a role in modulating recurvature longitude (Colbert & Soden, 2012). The Rossby wave pattern into which cyclones recurve and interaction between a cyclone and wave train during extratropical transition events can impact the evolution of storms (Laurila et al., 2019; Pantillon et al., 2013). Following extratropical transition, cyclones may propagate eastward under the influence of an upstream trough (Evans et al., 2017; Harr et al., 2008). For both landfall domains, the composite "asym_CC" tracks show a sharp transition from northward to eastward propagation, whereas "sym_WC" systems follow smoother recurvature (Figure 9), indicating continued southerly steering into a midlatitude block is associated with their retention of tropical characteristics. Cyclone-flow interactions may also operate in the opposite direction: a transitioning cyclone may influence both the upstream trough and amplify the ridge-trough pattern immediately downstream (Keller et al., 2019). The relative position (i.e., phasing) between a cyclone and the upstream trough affects the cyclone's post-transition reintensification (Keller et al., 2019). A reintensified, transitioned cyclone may contribute to downstream ridge-building, and thereby reinforce a preexisting midlatitude block. These interactions between the post-tropical structural evolution of storms, particularly whether extratropical transition is completed, and the midlatitude environment are therefore key in determining whether storms can propagate to Europe. Future work will further examine the midlatitude steering and synoptic conditions conducive to warm-core and cold-core lifecycles of tropical-origin cyclones, which may, in turn, yield improved landfall predictability based on a cyclone's midlatitude evolution.

4. Conclusions

We examined historical variability, lifecycles, and landfall characteristics of North Atlantic tropical and post-tropical cyclones across seven reanalysis data sets and HURDAT2 observations, focusing our analysis on systems that impacted two landfall domains: Northeast North America and Europe. This paper demonstrates that tropical-origin cyclone landfalls over the midlatitudes are not exceptional events, but instead a robust seasonal feature of North Atlantic storminess, which is highly consistent across seven reanalysis data sets. As such, these systems are an integral part of both current and future North Atlantic storm risk throughout the annual cycle.

The frequency of extratropical transition occurrence across the North Atlantic basin increases in most, but not all, reanalyses since 1979 (1958 for JRA55; 1980 for MERRA2), but there are no statistically significant

trends when considering all tropical-origin cyclones that make landfall. These interreanalysis differences highlight uncertainty due to changes in assimilated observations as well as differing data-assimilation schemes and forecast model formulations across reanalyses. Trend uncertainties due to the choice of tropical cyclone identification and phase-space criteria also necessitate further analysis. Yanase et al. (2014) identified transitioning tropical cyclones based on phase-space parameters, avoiding the need for the objective tropical cyclone identification. Using cyclone phase-space criteria to identify tropical cyclones may yield different results than the objective identification criteria (cyclogenesis and relative vorticity structure) used in this study. Although phase-space parameters may allow for better separation of tropical and subtropical cyclones, such differences would be seen primarily in weaker systems. Future work should seek to better understand these uncertainties.

Our analysis reveals clear distinctions between warm-core and cold-core landfalls. For warm-core landfalls, including warm-seclusion systems, peak v_{max} occurs at or near to landfall. Therefore, rather than being simply remnant lows, cyclones which retain or redevelop tropical-cyclone structural characteristics are climatologically more hazardous systems than tropical cyclones that undergo extratropical transition. For cold-core landfalls, peak v_{max} is lower and occurs after landfall over Northeast North America and Europe, a different storm-hazard profile. Additionally, reanalyses provide evidence for distinct warm-core and cold-core track recurvature, at least over the last four decades. For NENAm, cyclones that make landfall as cold-core systems, typically graze the United States' eastern coastline, but warm-core systems recurve farther east. For Europe, despite disparate recurvature behaviors, tropical-origin cyclones make landfall at ~55°N irrespective of core structure. However, reanalysis data sets are currently too short to assess both decadal variability and long-term trends in track and landfall locations. To understand long-term variability in North Atlantic tropical-origin cyclone risk, the forthcoming extension to ERA5 offers potential, notwithstanding uncertainties due to historical changes in observation coverage and quality. Additionally, recent developments in twentieth-century reanalysis products also offer potential, but only surface observations are assimilated in these data sets and their horizontal resolutions—typically 70–100 km—are too low to properly represent a cyclone's thermal structure (Hodges et al., 2017; Murakami, 2014; Schenkel & Hart, 2012). Therefore, complementary studies of centennial-length, high-resolution global climate model integrations will certainly be needed, and our results provide a robust baseline against which the credibility of such simulations may be evaluated more comprehensively, based on identical tracking and identification methodologies.

Finally, observational reconnaissance and monitoring of tropical-origin systems by operational weather centers across Europe will be prudent—now and in future. Moreover, the impacts of cyclones which undergo extratropical transition, while weaker, may be less localized around the storm center, owing to their frontal structure and larger horizontal size, and may also be more variable spatiotemporally compared with warm-core systems. There is a clear need for analysis of two-dimensional, impact-relevant quantities to complement the pointwise Lagrangian analyses herein. Over Europe, observed hurricane landfalls (e.g., Hurricane Vince in 2005) are historically rare, yet model projections (Baatsen et al., 2015; Haarsma et al., 2013) point to more frequent midlatitude landfalls of systems with tropical-cyclone-like hazards. Warm-core systems are simulated by global climate models with atmospheric horizontal grid resolutions of ~¼° (Baatsen et al., 2015). Such resolutions are now routinely feasible in global climate integrations, and a recent evaluation of high-resolution model simulations of the period 1950–2050 (Roberts et al., 2020b) revealed uncertainty in the future trend of basin-wide North Atlantic tropical cyclone frequency, highlighting the need for future modeling efforts. Establishing the fidelity of projections requires well-evaluated models. This study therefore satisfies a need for objective and systematic characterization of both tropical and post-tropical cyclones in the midlatitudes across multiple reanalyses, including their relationship with intensity metrics, which will be valuable not only in model assessment, but also in framing the key climate-risk questions.

Conflict of Interest

The authors declare no competing financial or other interests.

Data Availability Statement

HURDAT2 data (version 01/05/2018 obtained from aoml.noaa.gov/hrd/hurdat); all reanalysis data sets for tropical-cyclone tracking (vorticity, wind fields, sea-level pressure) and cyclone phase-space analysis (geopotential) are available from rda.ucar.edu or disc.gsfc.nasa.gov. All reanalyzes are freely accessible. TRACK is available for use with permission (see nerc-essc.ac.uk/~kih/TRACK/Track.html). Data analysis and visualization code are available from the lead author upon request (hrcm.ceda.ac.uk/contact).

Acknowledgments
A. J. Baker received financial support from the PRIMAVERA project (European Commission Horizon2020 Grant Agreement No. 641727). The authors thank Reindert J. Haarsma (Royal Netherlands Meteorological Institute) and Benoît Vannière (National Centre for Atmospheric Science and Department of Meteorology, University of Reading) for helpful discussions, and are equally grateful to the editor and to Ron McTaggart-Cowan (Canadian Meteorological Centre) and two anonymous reviewers whose recommendations improved this paper.

References

Baatsen, M., Haarsma, R. J., Van Delden, A. J., & de Vries, H. (2015). Severe autumn storms in future Western Europe with a warmer Atlantic Ocean. *Climate Dynamics*, *45*, 949–964. https://doi.org/10.1007/s00382-014-2329-8

Bieli, M., Camargo, S. J., Sobel, A. H., Evans, J. L., & Hall, T. (2019). A global climatology of extratropical transition. Part I: Characteristics across basins. *Journal of Climate*, *32*, 3557–3582. https://doi.org/10.1175/jcli-d-17-0518.1

Bieli, M., Sobel, A. H., Camargo, S. J., Murakami, H., & Vecchi, G. A. (2020). Application of the cyclone phase space to extratropical transition in a global climate model. *Journal of Advances in Modeling Earth Systems*, *12*, e2019MS001878. https://doi.org/10.1029/2019MS001878

Blake, E. S., Kimberlain, T. B., Berg, R. J., Cangialosi, J. P., & Beven, J. L. II (2013). *National Hurricane Center tropical cyclone report*. (Hurricane Sandy (AL182012). Retrieved from https://www.nhc.noaa.gov/data/tcr/AL182012_Sandy.pdf

Colbert, A. J., & Soden, B. J. (2012). Climatological variations in North Atlantic tropical cyclone tracks. *Journal of Climate*, *25*, 657–673. https://doi.org/10.1175/jcli-d-11-00034.1

Daloz, A. S., & Camargo, S. J. (2018). Is the poleward migration of tropical cyclone maximum intensity associated with a poleward migration of tropical cyclone genesis? *Climate Dynamics*, *50*, 705–715. https://doi.org/10.1007/s00382-017-3636-7

Dee, D. P., Uppala, S. M., Simmons, A. J., Berrisford, P., Poli, P., Kobayashi, S., et al. (2011). The ERA-Interim reanalysis: Configuration and performance of the data assimilation system. *Quarterly Journal of the Royal Meteorological Society*, *137*, 553–597. https://doi.org/10.1002/qj.828

Dekker, M. M., Haarsma, R. J., Vries, H. D., Baatsen, M., & Delden, A. J. V. (2018). Characteristics and development of European cyclones with tropical origin in reanalysis data. *Climate Dynamics*, *50*, 445–455. https://doi.org/10.1007/s00382-017-3619-8

Delgado, S., Landsea, C. W., & Willoughby, H. (2018). Reanalysis of the 1954–63 Atlantic Hurricane Seasons. *Journal of Climate*, *31*, 4177–4192. https://doi.org/10.1175/jcli-d-15-0537.1

Evans, C., Wood, K. M., Aberson, S. D., Archambault, H. M., Milrad, S. M., Bosart, L. F., et al. (2017). The extratropical transition of tropical cyclones. Part I: Cyclone evolution and direct impacts. *Monthly Weather Review*, *145*, 4317–4344. https://doi.org/10.1175/mwr-d-17-0027.1

Haarsma, R. J., Hazeleger, W., Severijns, C., de Vries, H., Sterl, A., Bintanja, R., et al. (2013). More hurricanes to hit western Europe due to global warming. *Geophysical Research Letters*, *40*, 1783–1788. https://doi.org/10.1002/grl.50360

Haarsma, R. J., Roberts, M. J., Vidale, P. L., Senior, C. A., Bellucci, A., Bao, Q., et al. (2016). High resolution model intercomparison project (HighResMIP v1.0) for CMIP6. *Geoscientific Model Development*, *9*, 4185–4208. https://doi.org/10.5194/gmd-9-4185-2016

Hagen, A. B., Strahan-Sakoskie, D., & Luckett, C. (2012). A reanalysis of the 1944–53 Atlantic Hurricane Seasons—The first decade of aircraft reconnaissance*. *Journal of Climate*, *25*, 4441–4460. https://doi.org/10.1175/jcli-d-11-00419.1

Harr, P. A., Anwender, D., & Jones, S. C. (2008). Predictability associated with the downstream impacts of the extratropical transition of tropical cyclones: Methodology and a case study of Typhoon Nabi (2005). *Monthly Weather Review*, *136*, 3205–3225. https://doi.org/10.1175/2008mwr2248.1

Hart, R. E. (2003). A cyclone phase space derived from thermal wind and thermal asymmetry. *Monthly Weather Review*, *131*, 585–616. https://doi.org/10.1175/1520-0493(2003)131<0585:acpsdf>2.0.co;2

Hart, R. E., & Evans, J. L. (2001). A climatology of the extratropical transition of Atlantic tropical cyclones. *Journal of Climate*, *14*, 546–564. https://doi.org/10.1175/1520-0442(2001)014<0546:acotet>2.0.co;2

Hersbach, H., Bell, B., Berrisford, P., Hirahara, S., Horányi, A., Muñoz-Sabater, J., et al. (2020). The ERA5 global reanalysis. *Quarterly Journal of the Royal Meteorological Society*, *146*, 1999–2049. https://doi.org/10.1002/qj.3803

Hodges, K., Cobb, A., & Vidale, P. L. (2017). How well are tropical cyclones represented in reanalysis datasets? *Journal of Climate*, *30*, 5243–5264. https://doi.org/10.1175/jcli-d-16-0557.1

Hodges, K. I. (1995). Feature tracking on the unit sphere. *Monthly Weather Review*, *123*, 3458–3465. https://doi.org/10.1175/1520-0493(1995)123<3458:ftotus>2.0.co;2

Hodges, K. I. (1996). Spherical nonparametric estimators applied to the UGAMP model integration for AMIP. *Monthly Weather Review*, *124*, 2914–2932. https://doi.org/10.1175/1520-0493(1996)124<2914:sneatt>2.0.co;2

Hodges, K. I. (1999). Adaptive constraints for feature tracking. *Monthly Weather Review*, *127*, 1362–1373. https://doi.org/10.1175/1520-0493(1999)127<1362:acfft>2.0.co;2

Jones, S. C., Harr, P. A., Abraham, J., Bosart, L. F., Bowyer, P. J., Evans, J. L., et al. (2003). The extratropical transition of tropical cyclones: Forecast challenges, current understanding, and future directions. *Weather and Forecasting*, *18*, 1052–1092. https://doi.org/10.1175/1520-0434(2003)018<1052:tetotc>2.0.co;2

Jung, C., & Lackmann, G. M. (2019). Extratropical transition of Hurricane Irene (2011) in a changing climate. *Journal of Climate*, *32*, 4847–4871. https://doi.org/10.1175/jcli-d-18-0558.1

Keller, J. H., Grams, C. M., Riemer, M., Archambault, H. M., Bosart, L., Doyle, J. D., et al. (2019). The extratropical transition of tropical cyclones. Part II: Interaction with the midlatitude flow, downstream impacts, and implications for predictability. *Monthly Weather Review*, *147*, 1077–1106. https://doi.org/10.1175/mwr-d-17-0329.1

Kobayashi, S., Ota, Y., Harada, Y., Ebita, A., Moriya, M., Onoda, H., et al. (2015). The JRA-55 reanalysis: General specifications and basic characteristics. *Journal of the Meteorological Society of Japan*, *93*, 5–48. https://doi.org/10.2151/jmsj.2015-001

Kossin, J. P., Emanuel, K. A., & Vecchi, G. A. (2014). The poleward migration of the location of tropical cyclone maximum intensity. *Nature*, *509*, 349–352. https://doi.org/10.1038/nature13278

Landsea, C. W., & Franklin, J. L. (2013). Atlantic hurricane database uncertainty and presentation of a new database format. *Monthly Weather Review*, *141*, 3576–3592. https://doi.org/10.1175/mwr-d-12-00254.1

Laurila, T. K., Sinclair, V. A., & Gregow, H. (2019). The extratropical transition of Hurricane Debby (1982) and the subsequent development of an intense windstorm over Finland. *Monthly Weather Review*, *148*, 377–401. https://doi.org/10.1175/mwr-d-19-0035.1

Liu, M., Vecchi, G. A., Smith, J. A., & Murakami, H. (2017). The present-day simulation and twenty-first-century projection of the climatology of extratropical transition in the North Atlantic. *Journal of Climate*, *30*, 2739–2756. https://doi.org/10.1175/jcli-d-16-0352.1

Mei, W., Kamae, Y., Xie, S.-P., & Yoshida, K. (2019). Variability and predictability of North Atlantic hurricane frequency in a large ensemble of high-resolution atmospheric simulations. *Journal of Climate*, *32*, 3153–3167. https://doi.org/10.1175/jcli-d-18-0554.1

Molod, A., Takacs, L., Suarez, M., & Bacmeister, J. (2015). Development of the GEOS-5 atmospheric general circulation model: Evolution from MERRA to MERRA2. *Geoscientific Model Development*, *8*, 1339–1356. https://doi.org/10.5194/gmd-8-1339-2015

Murakami, H. (2014). Tropical cyclones in reanalysis data sets. *Geophysical Research Letters*, *41*, 2133–2141. https://doi.org/10.1002/2014GL059519

Onogi, K., Tsutsui, J., Koide, H., Sakamoto, M., Kobayashi, S., Hatsushika, H., et al. (2007). The JRA-25 reanalysis. *Journal of the Meteorological Society of Japan*, *85*, 369–432. https://doi.org/10.2151/jmsj.85.369

Pantillon, F., Chaboureau, J.-P., Lac, C., & Mascart, P. (2013). On the role of a Rossby wave train during the extratropical transition of Hurricane Helene (2006). *Quarterly Journal of the Royal Meteorological Society*, *139*, 370–386. https://doi.org/10.1002/qj.1974

Rienecker, M. M., Suarez, M. J., Gelaro, R., Todling, R., Bacmeister, J., Liu, E., et al. (2011). MERRA: NASA's modern-era retrospective analysis for research and applications. *Journal of Climate*, *24*, 3624–3648. https://doi.org/10.1175/jcli-d-11-00015.1

Roberts, M. J., Camp, J., Seddon, J., Vidale, P. L., Hodges, K., Vannière, B., et al. (2020b). Projected future changes in tropical cyclones using the CMIP6 HighResMIP multimodel ensemble. *Geophysical Research Letters*, *47*, e2020GL088662. https://doi.org/10.1029/2020GL088662

Roberts, M. J., Camp, J., Seddon, J., Vidale, P. L., Hodges, K., Vanniere, B., et al. (2020a). Impact of model resolution on tropical cyclone simulation using the HighResMIP-PRIMAVERA multimodel ensemble. *Journal of Climate*, *33*, 2557–2583. https://doi.org/10.1175/jcli-d-19-0639.1

Saha, S., Moorthi, S., Wu, X., Wang, J., Nadiga, S., Tripp, P., et al. (2014). The NCEP climate forecast system version 2. *Journal of Climate*, *27*, 2185–2208. https://doi.org/10.1175/jcli-d-12-00823.1

Schenkel, B. A., & Hart, R. E. (2012). An examination of tropical cyclone position, intensity, and intensity life cycle within atmospheric reanalysis datasets. *Journal of Climate*, *25*, 3453–3475. https://doi.org/10.1175/2011jcli4208.1

Schreck, C. J. III, Knapp, K. R., & Kossin, J. P. (2014). The impact of best track discrepancies on global tropical cyclone climatologies using IBTrACS. *Monthly Weather Review*, *142*, 3881–3899. https://doi.org/10.1175/mwr-d-14-00021.1

Sharmila, S., & Walsh, K. J. E. (2018). Recent poleward shift of tropical cyclone formation linked to Hadley cell expansion. *Nature Climate Change*, *8*, 730–736. https://doi.org/10.1038/s41558-018-0227-5

Stewart, S. R. (2018). *National Hurricane Center tropical cyclone report*. Hurricane Ophelia (AL172017). Retrieved from www.nhc.noaa.gov/data/tcr/AL172017_Ophelia.pdf

Studholme, J., & Gulev, S. (2018). Concurrent changes to Hadley circulation and the meridional distribution of tropical cyclones. *Journal of Climate*, *31*, 4367–4389. https://doi.org/10.1175/jcli-d-17-0852.1

Studholme, J., Hodges, K. I., & Brierley, C. M. (2015). Objective determination of the extratropical transition of tropical cyclones in the Northern Hemisphere. *Tellus A: Dynamic Meteorology and Oceanography*, *67*, 24474. https://doi.org/10.3402/tellusa.v67.24474

Vecchi, G. A., & Knutson, T. R. (2008). On estimates of historical North Atlantic tropical cyclone activity. *Journal of Climate*, *21*, 3580–3600. https://doi.org/10.1175/2008jcli2178.1

Vecchi, G. A., & Knutson, T. R. (2011). Estimating annual numbers of Atlantic hurricanes missing from the HURDAT database (1878–1965) using ship track density. *Journal of Climate*, *24*, 1736–1746. https://doi.org/10.1175/2010jcli3810.1

Velden, C., Harper, B., Wells, F., Beven, J. L., Zehr, R., Olander, T., et al. (2006). The Dvorak tropical cyclone intensity estimation technique: A satellite-based method that has endured for over 30 years. *Bulletin of the American Meteorological Society*, *87*, 1195–1210. https://doi.org/10.1175/bams-87-9-1195

Wessel, P., & Smith, W. H. F. (1996). A global, self-consistent, hierarchical, high-resolution shoreline database. *Journal of Geophysical Research*, *101*, 8741–8743. https://doi.org/10.1029/96JB00104

Yanase, W., Niino, H., Hodges, K., & Kitabatake, N. (2014). Parameter spaces of environmental fields responsible for cyclone development from tropics to extratropics. *Journal of Climate*, *27*, 652–671. https://doi.org/10.1175/jcli-d-13-00153.1

Yang, G.-Y., Methven, J., Woolnough, S., Hodges, K., & Hoskins, B. (2018). Linking African easterly wave activity with equatorial waves and the influence of Rossby waves from the southern hemisphere. *Journal of the Atmospheric Sciences*, *75*, 1783–1809. https://doi.org/10.1175/jas-d-17-0184.1

Zarzycki, C. M., Thatcher, D. R., & Jablonowski, C. (2017). Objective tropical cyclone extratropical transition detection in high-resolution reanalysis and climate model data. *Journal of Advances in Modeling Earth Systems*, *9*, 130–148. https://doi.org/10.1002/2016MS000775